Small-Scale Spectrum Aggregation and Sharing

Paweł Kryszkiewicz, *Member, IEEE*, Adrian Kliks, *Senior Member, IEEE*,
and Hanna Bogucka, *Senior Member, IEEE*

***Abstract*— New spectrum bands together with flexible spectrum management are treated as one of the key technical enablers for achievement of the so-called key-performance indicators defined for 5G wireless networks. In this paper, we deal with the small-scale spectrum aggregation and sharing, where a set of even very narrow and disjoint frequency bands closely located on the frequency axis can be utilized simultaneously. We first discuss how such a scheme can be applied to various multicarrier systems, focusing on the non-contiguous orthogonal frequency division multiplexing and non-contiguous filter-bank multicarrier technique. We propose an interference model that takes into account the limitations of both transmitter and receiver frequency selectivity, and apply it to our 5G link-optimization framework, what differentiates our work from other standard approaches to link adaptation. We present the results of hardware experiments to validate assumed theoretical interference models. Finally, we solve the optimization problem subject to the constraints of maximum interference induced to the protected legacy systems (GSM and UMTS). Results confirm that small-scale spectrum aggregation can provide high throughput even when the 5G system operates in a dense heterogeneous network.**

***Index Terms*— Spectrum sharing, spectrum aggregation, non-contiguous multicarrier systems, co-channel and adjacent-channel interference.**

I. Introduction

NUMEROUS forecasts and statistical analyses confirm the continuous growth of mobile traffic that in the near future will reach the impressive level of tens of exabytes per month [1]. Such a trend has been reflected in the definitions of the so-called Key Performance Indicators (KPIs) which shape the requirements for the next generation wireless systems. Even 1000 fold increase of traffic volume is anticipated comparing to 4G Long Term Evolution - Advanced (LTE-A) systems while constraints on allowable latency or energy consumption will be more demanding [2], [3]. Practical implementation of such challenging goals will require identification of technically advanced solutions, which can be classified to three groups, providing: *more spectrum, more spectral- and more spatial efficiency* as identified in [4]. It has been recognized that advanced spectrum sharing and aggregation can be the enablers for such 5G networks [5]–[7]. In this work, we focus on flexible and efficient aggregation and sharing of licensed spectrum.

Efficient and flexible utilization of frequency bands below 6 GHz requires accurate interference management, especially in the scenarios of heterogeneous wireless systems coexistence. One of the options is the assignment of spectrum bands currently unused by the licensed (primary) users to the unlicensed (secondary) users, as in the cognitive radio concept [8]. However, the problem of effective coexistence of different systems can be analyzed from another perspective: mobile network operators (MNOs) can make a business decision to migrate from one (older) technology (e.g., GSM or UMTS) to another one (such as LTE-A, or to a future 5G technology). What is characteristic for both scenarios is the relation between bandwidths of the legacy and new wireless systems: GSM transmission can be treated as *narrowband*, whereas LTE-A and 5G systems can operate on much broader frequency bands (up to 100 MHz). Thus, should the GSM or UMTS users be active, it can happen that the potentially wide vacant spectrum will be split into a number of unused but narrower spectrum resources. Such an observation leads us to the concept of small-scale spectrum aggregation and sharing scheme, which we have initially presented in [9].

Analogously to the carrier aggregation (CA) approach, we suggest that even narrow frequency fragments which are currently unused, and which are interleaved with the existing signals, can be effectively assigned to users (user equipment, UE) for data transmission. Contrarily to the classic CA where a well defined resource block, or a fixed set of carriers (of the band of some MHz) can be utilized by one user (or data stream), here, we focus on the small-scale going down theoretically to the size of resource elements of some kHz, which can be achieved thanks to the non-contiguous (NC) multicarrier (MC) techniques. As in any coexistence scenario, it is the mutual interference that plays the crucial role. Should the narrow frequency bands be aggregated, advanced interference management algorithms have to be implemented as well.

In the NC-MC transmission, at least one set of subcarriers is not used, as it is occupied by other systems (e.g., legacy UMTS or GSM) which have to be protected from interference. In the considered context of spectrum sharing and systems coexistence, the problem of generated interference has to be analyzed twofold. First, backward compatibility has to be guaranteed, i.e., the Protected Systems (PSs) should not be distorted by the introduced NC-MC transmission. Here, one needs to consider technical imperfections of the devices: selectivity of the reception filters and non-ideal spectrum emission masks. Second, newer 5G devices will observe a certain level of

Manuscript received April 29, 2016; revised August 4, 2016; accepted August 28, 2016. Date of publication September 1, 2016; date of current version October 13, 2016. This work was supported by the EU H2020 Project COHERENT under Contract 671639.

The authors are with the Faculty of Electronics and Telecommunication, Poznan University of Technology, 60-965 Poznan, Poland (e-mail: pawel.kryszkiewicz@put.poznan.pl; adrian.kliks@put.poznan.pl; hanna.bogucka@put.poznan.pl).

Color versions of one or more of the figures in this paper are available online at http://ieeexplore.ieee.org.

Digital Object Identifier 10.1109/JSAC.2016.2604999

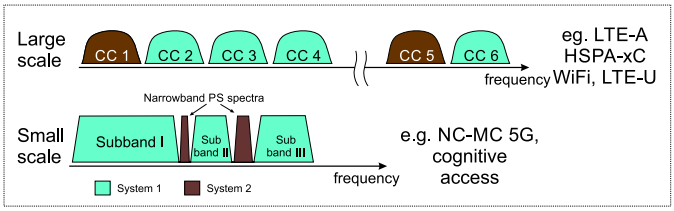

Fig. 1. Large and small scale spectrum aggregation and sharing.

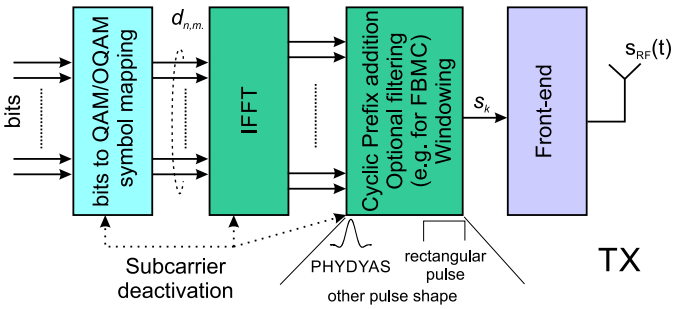

Fig. 2. Block diagram of the generic non-contiguous multicarrier TX.

interference originating from the legacy systems. In our analysis, we consider these aspects in detail. We claim that there are benefits for various stakeholders from the application of small-scale spectrum sharing and aggregation despite practical system limitations.

The novelty of this position paper is the following. First, we present the concept of NC-MC utilization in 5G system considering generated and observed interference. Then, the analytical model of interference is derived, taking practical characteristics of the transmit and reception filters into account. (Typically, the reception filter characteristic is not considered in derivations, although it influences significantly the interference power gathered by the wireless receiver (RX).) It is then validated by real-world measurements. Next, we define and solve the 5G-system rate optimization problem using this interference model, subject to efficient protection of the incumbents. The low-complex algorithm for finding this solution is also provided. Finally, the proposed scheme is evaluated by means of computer simulations, in which mobility of users and imperfect channel state information are assumed at the 5G Base Station (BS).

In Sec. II, we present the concept of small-scale spectrum aggregation and sharing. We analyze the cross-interference problem in a coexistence framework of 5G NC-MC transmission with a legacy system in Sec. III. Within this framework, we define and solve the NC-MC system-rate optimization problem in Sec. IV. In Sec. V, we evaluate our concept for two cases: coexistence of a 5G NC-MC system with either GSM or UMTS. The paper is concluded in Sec. VI.

II. Non-Contiguous Multicarrier Schemes as the Small-Scale Spectrum Aggregation Mechanism

Spectrum agreggation refers to making use of discontinuous frequency bands, and thus, to utilizing the broader electromagnetic frequency band. A specific instantiation of this concept tailored to the 4G networks is the mentioned carrier aggregation. There, spectrum utilized by one user is a multiple of component carriers (CC) which jointly create non-contiguous frequency segments. Solutions that use multiple physical carriers applied to LTE-A or multiple-carrier (multiple-cell) HSPA (HSPA-xC) systems are exemplifications of this approach, and are illustrated in the upper part of Fig. 1. As a complement to this, small-scale spectrum aggregation can be considered, as illustrated in the bottom of this figure, where instead of CCs, frequency segments of arbitrary (possibly much narrower) bandwidths can be assigned to particular users or systems. For example, an operator may share own-licensed spectrum among various technologies (e.g., GSM and 5G, LTE Release 8 and 5G, WiMAX with 5G, etc.).

In the following, we briefly discuss how the non-contiguous-spectrum approach could be applied to various modulations and channel access schemes, such as orthogonal frequency division multiplexing (OFDM) and filter-bank multicarrier (FBMC) scheme, leading to the NC-OFDM and NC-FBMC schemes, accordingly.

The NC-MC transmission scheme can be realized by deactivating certain sets of subcarriers, and optionally by applying some additional signal processing in order to respect the allowable interference level at the frequency-neighboring system receivers [10]. Figure 2 shows a generic NC-MC transmitter (TX), where data-bits are mapped to QAM/PSK complex symbols and fed to N_{d} inputs of N-size IFFT ($N_{\mathrm{d}} \leq N$). The set of N_{d} occupied subcarriers indices $\mathbf{I}_{\mathrm{DC}} \subset \left\{-\frac{N}{2}, \ldots, \frac{N}{2}-1\right\}$ is controlled by a dedicated steering block. The other inputs are modulated by 0 values (usually, these are subcarriers overlapping PS band). The complex symbol (zero or QAM/PSK) modulating the n-th subcarrier ($n \in \left\{-\frac{N}{2}, \ldots, \frac{N}{2}-1\right\}$) in the m-th MC symbol is denoted as $d_{n,m}$. The samples at the output of IFFT are further processed, e.g., by digital filtering, cyclic prefix addition, creating time-domain samples s_k. Finally, the baseband signal is converted from discrete to analogue form, shifted to the radio-frequency (RF) band, and amplified in the front-end, resulting in time-domain signal $s_{\mathrm{RF}}(t)$. The discrete signals are sampled with frequency $f_s = N\Delta f$, where Δf defines the subcarrier spacing.

The discrete NC-MC signal generated in the way presented above can be described as:

$$s_k = \sum_{m\in\mathbb{Z}} \sum_{n=-\frac{N}{2}}^{\frac{N}{2}-1} d_{n,m} \overbrace{\phi[k-mM]\, e^{\left(\iota \frac{2\pi n}{N}(k-mM)\right)}}^{\phi_{n,m}[k]} \tag{1}$$

where $\phi_{n,m}[k]$ is the original pulse shape $\phi[k]$ shifted in time and in frequency by mM samples and n subcarriers respectively, $\mathbb{Z}$ is the set of integers, and $\iota^2 = -1$. In general, M and Δf can be understood as the time and frequency distance between two consecutive and adjacent pulses on the time-frequency plane. In our further analysis, we limit the time-span to one multicarrier symbol, so that index m in $d_{n,m}$ is omitted. In such a case, the NC-MC symbol frequency representation $S(\omega)$ at normalized pulsation $\omega \in \langle -\pi, \pi \rangle$ can be obtained by Fourier transformation of a time domain

signal s_k as in [11] and [12]: $S(\omega) = \sum_{n=-\frac{N}{2}}^{\frac{N}{2}-1} d_n S^{\mathrm{TX}}(\omega, n)$, where $S^{\mathrm{TX}}(\omega, n)$ is the n-th subcarrier frequency response. Obviously, in the case of the ideal transmit filter, i.e., having ones in its frequency response pass band and zeroes otherwise, the n-th subcarrier does not cause interference outside its band, so that $\left|S^{\mathrm{TX}}(\omega, n)\right|^2 = \Pi\left(\frac{N}{2\pi}\left(\omega - 2\pi\frac{n}{N}\right)\right)$ where $\Pi(x)$ is a rectangular function equal 1 for $x \in (-0.5; 0.5)$, 0 otherwise. At the NC-MC receiver, the dual pulse-shaping filtering is applied. In the case of signal perfect-reconstruction, the RX filter characteristic is a complex conjugate of the TX filter, thus, $|S^{\mathrm{RX}}(\omega, n)| = |S^{\mathrm{TX}}(\omega, n)|$.

In the following we exemplify these observations to the specific NC-MC systems.

A. Scheme 1: NC-OFDM

If we consider the NC-OFDM technique, $\phi[k]$ is the sampled rectangular pulse (it equals 1 for $k \in \{-N_{\mathrm{CP}}, \ldots, N-1\}$, and zeros otherwise), and at the output of IFFT, N_{CP} samples of cyclic prefix (CP) are inserted. The output samples s_k $(k = -N_{\mathrm{CP}}, \ldots, N-1)$ are defined as:

$$s_k = \sum_{n=-\frac{N}{2}}^{\frac{N}{2}-1} d_n e^{\left(\imath\frac{2\pi n}{N}k\right)}. \tag{2}$$

Moreover, the normalized frequency representation of the n-th subcarrier $S^{\mathrm{TX}}(\omega, n)$, in case of the NC-OFDM signal, can be defined for digital implementation similarly as in [13]:

$$S^{\mathrm{TX}}_{\mathrm{OFDM}}(\omega, n) = \frac{1}{\sqrt{N(N+N_{\mathrm{CP}})}} e^{-\imath\left(\frac{\omega}{2}-\frac{\pi n}{N}\right)(N-N_{\mathrm{CP}}-1)} \cdot \frac{\sin\left(\left(\frac{\omega}{2}-\frac{\pi n}{N}\right)(N+N_{\mathrm{CP}})\right)}{\sin\left(\frac{\omega}{2}-\frac{\pi n}{N}\right)}. \tag{3}$$

As the sidelobes power of an NC-OFDM signal is naturally high, advanced signal processing can be applied for out-of-band emission (OOBE) power minimization, such as implementation of the so-called cancellation carriers (where dedicated subcarriers convey symbols adjusted for OOBE power reduction [10]) or time-domain windowing [13]. At the receiver, N out of $N + N_{\mathrm{CP}}$ symbol samples are used, thus the n-th subcarrier reception filter response equals:

$$S^{\mathrm{RX}}_{\mathrm{OFDM}}(\omega, n) = \frac{1}{N} e^{\imath\left(\frac{\omega}{2}-\frac{\pi n}{N}\right)(N-1)} \frac{\sin\left(\left(\frac{\omega}{2}-\frac{\pi n}{N}\right)N\right)}{\sin\left(\frac{\omega}{2}-\frac{\pi n}{N}\right)}. \tag{4}$$

B. Scheme 2: NC-FBMC

One of the candidates in the quest for the most promising modulation format for 5G networks is FBMC that is based on the offset QAM (and is denoted jointly as FBMC/OQAM). Its key features are: the lack of CP (thus improving the spectrum and energy efficiency) and the possibility of each subcarrier spectrum shaping. The comparison between OFDM and FBMC has been presented in [14], whereas an example of the FBMC implementation for an NC scheme can be found in [15]. The transmit signal can be represented as:

$$s_k = \sum_{n=-\frac{N}{2}}^{\frac{N}{2}-1} \left\{d_n^{\mathrm{RE}}\phi[k] + \imath d_n^{\mathrm{IM}}\phi[k - N/2]\right\} \imath^n e^{\left(\imath\frac{2\pi}{N}nk\right)}, \tag{5}$$

where d_n^{RE} and d_n^{IM} denote the real and imaginary part of complex data d_n, $k = 0, \ldots, KN + N/2 - 1$, and K is a positive integer called overlapping factor [16]. If we apply a widely considered PHYDYAS prototype filter [16] we have the following frequency response of the n-th subcarrier:

$$S^{\mathrm{TX}}_{\mathrm{FBMC}}(\omega, n) = \frac{1}{KN} \sum_{z=-(K-1)}^{K-1} H_{|z|} e^{-\imath\left(\omega - 2\pi\frac{n}{N} - 2\pi\frac{z}{KN}\right)\frac{KN-1}{2}} \cdot \frac{\sin\left(\left(\omega - \frac{2\pi n}{N} - \frac{z}{K}\right)\frac{KN}{2}\right)}{\sin\left(\left(\omega - \frac{2\pi n}{N} - \frac{z}{K}\right)\frac{1}{2}\right)}, \tag{6}$$

where H_z (for $z = 0, .., K-1$) are the filter-characteristic samples. The RX filter characteristic is the complex conjugate of the TX filter, thus, $|S^{\mathrm{RX}}_{\mathrm{FBMC}}(\omega, n)| = |S^{\mathrm{TX}}_{\mathrm{FBMC}}(\omega, n)|$.

C. Other Schemes

Note that there exist other multicarrier schemes that could be analyzed separately. Some of them are envisaged as possible candidates for new 5G waveforms: *a*. Generalized Frequency Division Multiplexing (GFDM) [17], where subcarriers can be non-orthogonal, *b*. Universal Filtered MultiCarrier (UMFC), where instead of per-subcarrier filtering the groups of subcarriers are processed (filtered) [18], *c*. Filtered-OFDM [19], *d*. Biorthogonal [20] or Non-Orthogonal FDM [21], where biorthognal or non-orthogonal wavefors are applied, *e*. Generalized Multicarrier (GMC) scheme, which relaxes most of the constraints known in multicarrier system design [22]. In all of these cases the non-contiguity property of the subcarriers can be directly applied. Thus, in our further analysis we limit our discussion to the two already presented waveforms treating them as the representatives of the broader family of MC systems.

III. Interference Analysis

Let us consider a generic downlink case,[1] where the future 5G wireless system will be deployed in the same area as other, already existing PSs that have to be protected from harmful interference. Such a situation is illustrated in Fig. 3, where in its upper part one can observe two systems - the PS and the new (spectrally-flexible) 5G one. The user equipment to be protected (PS UE) receives the signal from its system BS (with power attenuation $\alpha_{\mathrm{PS-PS}}$ and frequency frequency response $H_{\mathrm{PS-PS}}(f)$), and observes interference from the coexisting system (via the channel of power attenuation $\alpha_{\mathrm{5G-PS}}$ and frequency response $H_{\mathrm{5G-PS}}(f)$). Similarly, the 5G UE detects not only the wanted NC-MC signal from its BS (via the channel of power-attenuation $\alpha_{\mathrm{5G-5G}}$ and frequency response $H_{\mathrm{5G-5G}}(f)$), but also interfering signal from incumbent PS (passing the channel of power-attenuation $\alpha_{\mathrm{PS-5G}}$ and frequency response $H_{\mathrm{PS-5G}}(f)$). In Fig. 3a, the wanted signal is denoted by solid line, whereas interference - by dotted line.

Our considerations focus on maximization of the rate achieved in the 5G system while fully protecting the incumbent users, taking limitations caused by the non-ideal nature

[1] Analogous derivations can be repeated for the uplink case.

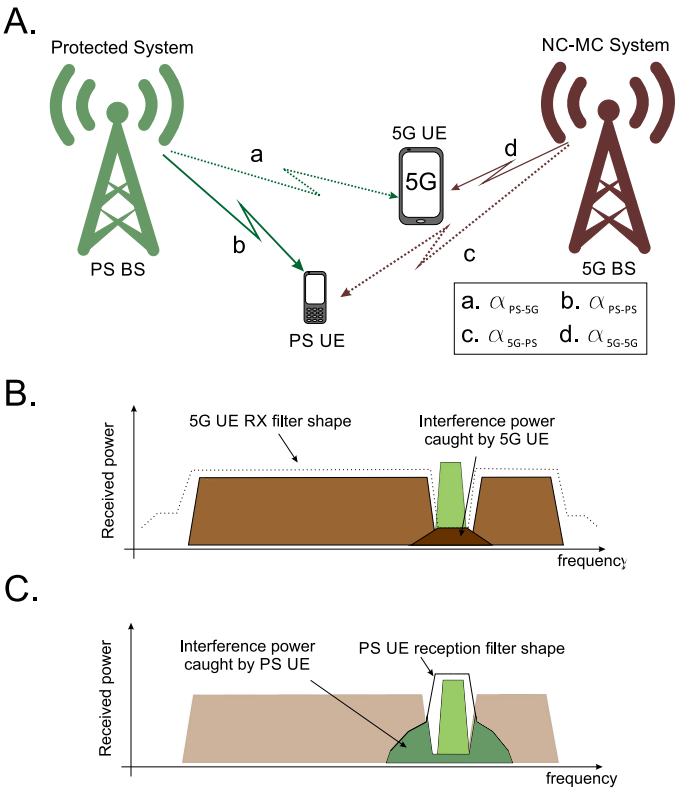

Fig. 3. Illustration of the coexistence of two wireless systems: the existing PS and the spectrally-flexible (applying NC-MC scheme) 5G system.

of the transmit and reception filters into account. Interference to PS results from the unwanted emission of the coexisting NC-MC TX out of the nominal band (known as OOBE, typically limited by the definition of so-called spectrum-emission-masks (SEM) or adjacent channel leakage ratio (ACLR)). Moreover, non-ideal RX filters with limited selectivity (described by the adjacent channel selectivity metric, ACS) gather the signal frequency components not only from the wanted frequency band, but also outside of it. These two cases are presented graphically in the bottom part of Fig. 3, and are denoted as *B* and *C*.

A. Generic Observations on Cross-Interference

If the power-attenuation of any considered downlink channel (including pathloss and antennas gains) is denoted by α, and the channel frequency response by $H_{\mathrm{TX-RX}}(f)$, the received interference power can be expressed as:

$$P_{\mathrm{I}} = \alpha \int_{-\infty}^{\infty} \Upsilon^{\mathrm{TX}}(f - f_c) \left| H^{\mathrm{RX}}(f - f_c) \right|^2 \cdot |H_{\mathrm{TX-RX}}(f - f_c)|^2 \, df, \tag{7}$$

where f_c is the center frequency of a considered system, $\Upsilon^{\mathrm{TX}}(f)$ is the power spectral density at the TX output (either PS or 5G base station) at frequency f and $H^{\mathrm{RX}}(f)$ is a frequency response of an RX filter (either PS or 5G terminal). As mentioned above, interference at a given frequency comes not only from the imperfect spectrum shaping at TX, but also from imperfect RX filter selectivity (reception filter "picks up" the interference being a part of the transmitted signal spectrum out of its nominal band). In our analysis we include both aspects, which is the novelty in this respect, as typically the reception filter selectivity is omitted in the derivations.

In the case of commonly used discrete-time representation of digital signals, the above equation simplifies to

$$P_{\mathrm{I}} = \frac{\alpha}{2\pi} \int_{-\pi}^{\pi} \Upsilon^{\mathrm{TX}}\left(\frac{\omega f_s}{2\pi}\right) \left| H^{\mathrm{RX}}\left(\frac{\omega f_s}{2\pi}\right) \right|^2 \cdot \left| H_{\mathrm{TX-RX}}\left(\frac{\omega f_s}{2\pi}\right) \right|^2 d\omega, \tag{8}$$

where $\omega \in \langle -\pi, \pi \rangle$ is pulsation and f_s is sampling frequency.

B. Interference From an NC-MC System

In case of an NC-MC system causing interference, all subcarriers are typically treated as independent, hence the total interference power can be defined as:

$$P_{\mathrm{I}} = \alpha \sum_{n=-\frac{N}{2}}^{\frac{N}{2}-1} P_{\mathrm{I}n}^{\mathrm{TX}}, \tag{9}$$

where the interference power caused by the n-th subcarrier $P_{\mathrm{I}n}^{\mathrm{TX}}$ equals:

$$P_{\mathrm{I}n}^{\mathrm{TX}} = P_n g_n = P_n \int_{-\pi}^{\pi} \left| S^{\mathrm{TX}}(\omega, n) \right|^2 \left| H^{\mathrm{RX}}\left(\frac{\omega f_s}{2\pi}\right) \right|^2 \cdot \left| H_{\mathrm{TX-RX}}\left(\frac{\omega f_s}{2\pi}\right) \right|^2 d\omega, \tag{10}$$

where P_n is the power allocated at the n-th subcarrier in the NC-MC transmitter and $S^{\mathrm{TX}}(\omega, n)$ is the n-th subcarrier frequency response at pulsation ω (as defined in (3) and (6) for OFDM and FBMC, respectively), and g_n is the integral result which can be interpreted as the coupling factor between the power transmitted on the n-th subcarrier observed at victim receiver's antenna and the effective interference power degrading victim's reception.

C. Interference to an NC-MC System

In the case of a victim NC-MC system (experiencing interference), formula (8) can be used, and the total interference power P_{I} is a sum of $P_{\mathrm{I}n}^{\mathrm{RX}}$ values (as in (9)). $P_{\mathrm{I}n}^{\mathrm{RX}}$ is the power of interference observed at the n-th subcarrier of the victim NC-MC receiver having the reception filter frequency response $S^{\mathrm{RX}}(\omega, n)$ (as discussed in Sec. II), and can be calculated as:

$$P_{\mathrm{I}n}^{\mathrm{RX}} = \int_{-\pi}^{\pi} \Upsilon^{\mathrm{TX}}\left(\frac{\omega f_s}{2\pi}\right) \left| S^{\mathrm{RX}}(\omega, n) \right|^2 \left| H_{\mathrm{TX-RX}}\left(\frac{\omega f_s}{2\pi}\right) \right|^2 d\omega. \tag{11}$$

IV. Problem Formulation

Once the interference model has been derived, let us consider throughput maximization for various 5G multicarrier schemes by adjusting the power transmitted by 5G BS on each subcarrier P_n ($n \in \mathbf{I}_{\mathrm{DC}}$) subject to constraints discussed later in this section. The optimization problem is defined so as to find the vector of the assigned powers $\mathbf{P} = \{P_n\}$ to maximize the Shannon data rate:

$$\mathbf{P}^* = \arg\max_{\mathbf{P}} \Delta f \chi \sum_{n\in\mathbf{I}_{\mathrm{DC}}} \log_2 \left(1 + \frac{\alpha_{5\mathrm{G}-5\mathrm{G}} P_n \left|H_{5\mathrm{G}-5\mathrm{G}}\left(\frac{nf_s}{N}\right)\right|^2}{FN_0\Delta f + \alpha_{\mathrm{PS}-5\mathrm{G}} P_{In}^{\mathrm{RX}}}\right) \tag{12}$$

where N_0 is a white noise power spectral density, and F is noise figure of the 5G NC-MC receiver. Moreover, χ is the rate-scaling factor accounting for the symbol duration extension (e.g. application of CP). It is equal to 1 in the ideal case (when no CP is used) or (NC-)FBMC, and equal to $N/(N + N_{\mathrm{CP}})$ in case of an OFDM or NC-OFDM system, which typically uses CP. Moreover, in the case of time-domain windowing applied to NC-OFDM [13], [23], each symbol of $N + N_{\mathrm{CP}}$ samples is additionally prolonged by N_{w} windowed samples giving $\chi = N/(N + N_{\mathrm{CP}} + N_{\mathrm{w}})$. In our optimization problem the following constraints have to be fulfilled.

a) PS QoS requirements: A spectrally-flexible 5G system should guarantee the Quality of Service (QoS) required by PS. If $\mathrm{SIR}_{\mathrm{min}}$ is the minimum signal-to-interference ratio (SIR) required by PS, then

$$\frac{P_{\mathrm{RX}}^{\mathrm{PS\ UE}}}{\sum_{n\in\mathbf{I}_{\mathrm{DC}}} \alpha_{5\mathrm{G}-\mathrm{PS}} P_n g_n} \geq \mathrm{SIR}_{\mathrm{min}}, \tag{13}$$

where $P_{\mathrm{RX}}^{\mathrm{PS\ UE}}$ is the useful signal power received by PS RX, and can be calculated as

$$P_{\mathrm{RX}}^{\mathrm{PS\ UE}} = \alpha_{PS-PS} \int_{-\pi}^{\pi} \Upsilon_{\mathrm{PS}}^{\mathrm{TX}}\left(\frac{\omega f_s}{2\pi}\right) \left|H_{\mathrm{PS}}^{\mathrm{RX}}\left(\frac{\omega f_s}{2\pi}\right)\right|^2 \cdot \left|H_{\mathrm{PS}-\mathrm{PS}}\left(\frac{\omega f_s}{2\pi}\right)\right|^2 d\omega, \tag{14}$$

$H_{\mathrm{PS}}^{\mathrm{RX}}\left(\frac{\omega f_s}{2\pi}\right)$ is a frequency response of a PS RX filter and $\Upsilon_{\mathrm{PS}}^{\mathrm{TX}}\left(\frac{\omega f_s}{2\pi}\right)$ is PSD of the PS signal at its transmitter.

b) Requirements on the NC-MC system transmit power: Next, a maximum power of the 5G NC-MC transmitter should be limited giving

$$\sum_{n\in\mathbf{I}_{\mathrm{DC}}} P_n \leq P_{\mathrm{max}}, \tag{15}$$

where P_{max} is a maximum allowed power of the 5G NC-MC transmitter. Finally, the power of each subcarrier must not be negative, i.e.,

$$\forall_{n\in\mathbf{I}_{\mathrm{DC}}} P_n \geq 0. \tag{16}$$

A. Problem Solution

Let us formulate an inequality constrained nonlinear optimization problem [24] as follows:

$$\mathbf{P}^* = \arg\min_{\mathbf{P}} \left[-\Delta f \chi \sum_{n\in\mathbf{I}_{\mathrm{DC}}} \log_2 \left(1 + \frac{\alpha_{5\mathrm{G}-5\mathrm{G}} P_n \left|H_{5\mathrm{G}-5\mathrm{G}}\left(\frac{nf_s}{N}\right)\right|^2}{FN_0\Delta f + \alpha_{\mathrm{PS}-5\mathrm{G}} P_{In}^{\mathrm{RX}}}\right)\right] \tag{17}$$

$$s.t. \sum_{n\in\mathbf{I}_{\mathrm{DC}}} \alpha_{5\mathrm{G}-\mathrm{PS}} P_n g_n - \frac{P_{\mathrm{RX}}^{\mathrm{PS\ UE}}}{\mathrm{SIR}_{\mathrm{min}}} \leq 0, \tag{18}$$

$$\sum_{n\in\mathbf{I}_{\mathrm{DC}}} P_n - P_{\mathrm{max}} \leq 0, \tag{19}$$

$$\forall_{n\in\mathbf{I}_{\mathrm{DC}}} - P_n \leq 0. \tag{20}$$

The Lagrangian function for this problem is:

$$\begin{aligned} J(P_n, \lambda, \mu, \mu_n) &= -\Delta f \chi \sum_{n\in\mathbf{I}_{\mathrm{DC}}} \log_2 \left(1 + \frac{\alpha_{5\mathrm{G}-5\mathrm{G}} P_n \left|H_{5\mathrm{G}-5\mathrm{G}}\left(\frac{nf_s}{N}\right)\right|^2}{FN_0\Delta f + \alpha_{\mathrm{PS}-5\mathrm{G}} P_{In}^{\mathrm{RX}}}\right) \\ &+ \mu \left(\sum_{n\in\mathbf{I}_{\mathrm{DC}}} \alpha_{5\mathrm{G}-\mathrm{PS}} P_n g_n - \frac{P_{\mathrm{RX}}^{\mathrm{PS\ UE}}}{\mathrm{SIR}_{\mathrm{min}}}\right) \\ &+ \lambda \left(\sum_{n\in\mathbf{I}_{\mathrm{DC}}} P_n - P_{\mathrm{max}}\right) + \sum_{n\in\mathbf{I}_{\mathrm{DC}}} \mu_n (-P_n), \end{aligned} \tag{21}$$

where μ_n, μ and λ are called Karush-Kuhn-Tucker (KKT) multipliers. The KKT necessary conditions used to solve this problem are:

$$\forall_{n\in\mathbf{I}_{\mathrm{DC}}} \frac{\partial J(P_n, \lambda, \mu, \mu_n)}{\partial P_n} = 0, \tag{22}$$

$$\mu \left(\sum_{n\in\mathbf{I}_{\mathrm{DC}}} \alpha_{5\mathrm{G}-\mathrm{PS}} P_n g_n - \frac{P_{\mathrm{RX}}^{\mathrm{PS\ UE}}}{\mathrm{SIR}_{\mathrm{min}}}\right) = 0, \tag{23}$$

$$\lambda \left(\sum_{n\in\mathbf{I}_{\mathrm{DC}}} P_n - P_{\mathrm{max}}\right) = 0, \tag{24}$$

$$\forall_{n\in\mathbf{I}_{\mathrm{DC}}} \mu_n (-P_n) = 0, \tag{25}$$

where $\forall_{n\in\mathbf{I}_{\mathrm{DC}}} \mu_n \geq 0$, $\mu \geq 0$ and $\lambda \geq 0$. The result of (22) is

$$P_n = \frac{\Delta f \chi}{\ln(2)\,(\lambda + \mu\alpha_{5\mathrm{G}-\mathrm{PS}} g_n - \mu_n)} - Q_n, \tag{26}$$

where

$$Q_n = \frac{FN_0\Delta f + \alpha_{\mathrm{PS}-5\mathrm{G}} P_{In}^{\mathrm{RX}}}{\alpha_{5\mathrm{G}-5\mathrm{G}} \left|H_{5\mathrm{G}-5\mathrm{G}}\left(\frac{nf_s}{N}\right)\right|^2} \tag{27}$$

that should be substituted to formulas (23)-(25) in order to find the multipliers values. For each constraint two possibilities have to be considered: the multiplier equals zero and the constraint is inactive or the multiplier is positive and the constraint is active. In the case of (25), when this constraint is

active for the n-th subcarrier (the power of the n-th subcarrier is zero), we obtain:

$$\mu_n = \lambda + \mu\alpha_{5\text{G}-\text{PS}}g_n - \frac{\Delta f\chi}{\ln(2)\,Q_n}. \tag{28}$$

In general, every combination of $N_\text{d}+2$ multipliers being active or inactive should be considered, i.e., $2^{N_\text{d}+2}$ cases. However, an algorithm presented below allows to decrease the number of combinations to be considered. For example, when the constraint (23) is active ($\mu > 0$ and interference power is constrained), and for n-th subcarrier μ_n has to be greater than zero, so the corresponding constraint (25) has to be *activated*, this will result in increased interference to PS. Thus, μ in (23) has to be still active. Let us first derive solutions for some special cases. Let us denote $\mathbf{I}_\text{cons}$ to be a set of size γ of indices n for which μ_n is positive, i.e., $P_n = 0$ ($\mathbf{I}_\text{cons} \subset \mathbf{I}_\text{DC}$). Thus, the following cases should be considered:

- If $\mu = 0$ and $\lambda \neq 0$, i.e., 5G BS is limited in the available power, the interference generated to PS UE is below the limit. Moreover, substitution of (26) into (24) together with $\mu_n = 0$ for $n \in \mathbf{I}_\text{DC} \setminus \mathbf{I}_\text{cons}$ and $P_n = 0$ for $n \in \mathbf{I}_\text{cons}$ results in:

$$\lambda = \frac{\Delta f\chi(N_d - \gamma)}{\ln(2)\left(\sum_{n\in\mathbf{I}_\text{DC}\setminus\mathbf{I}_\text{cons}} Q_n + P_\text{max}\right)}, \tag{29}$$

- If $\mu \neq 0$ and $\lambda = 0$, i.e., interference caused to PS UE prevents the 5G BS from obtaining the total transmit power P_max, (26) can be substituted to (23) together with $\mu_n = 0$ for $n \in \mathbf{I}_\text{DC} \setminus \mathbf{I}_\text{cons}$ and $P_n = 0$ for $n \in \mathbf{I}_\text{cons}$ that gives the following result:

$$\mu = \frac{\Delta f\chi(N_d - \gamma)}{\ln(2)\left(\sum_{n\in\mathbf{I}_\text{DC}\setminus\mathbf{I}_\text{cons}} \alpha_{5\text{G}-\text{PS}}g_n Q_n + \frac{P_\text{RX}^{\text{PS UE}}}{\text{SIR}_\text{min}}\right)}, \tag{30}$$

- If $\mu \neq 0$ and $\lambda \neq 0$, i.e., both interference generated to PS UE and power emitted by 5G TX have to be constrained, a set of two nonlinear equations obtained after substitution of (26) and $\mu_n = 0$ for $n \in \mathbf{I}_\text{DC} \setminus \mathbf{I}_\text{cons}$ and $P_n = 0$ for $n \in \mathbf{I}_\text{cons}$ into (23) and (24) has to be solved:

$$f_1(\mu,\lambda) = \sum_{n\in\mathbf{I}_\text{DC}\setminus\mathbf{I}_\text{cons}} \alpha_{5\text{G}-\text{PS}}g_n \cdot\left(\frac{\Delta f\chi}{\ln(2)\,(\lambda+\mu\alpha_{5\text{G}-\text{PS}}g_n)} - Q_n\right) - \frac{P_\text{RX}^{\text{PS UE}}}{\text{SIR}_\text{min}} = 0, \tag{31}$$

$$f_2(\mu,\lambda) = \sum_{n\in\mathbf{I}_\text{DC}\setminus\mathbf{I}_\text{cons}} \left(\frac{\Delta f\chi}{\ln(2)\,(\lambda+\mu\alpha_{5\text{G}-\text{PS}}g_n)} - Q_n\right) - P_\text{max} = 0. \tag{32}$$

Here, the Newton method can be applied as the required derivatives can be calculated as

$$\frac{\partial f_1(\mu,\lambda)}{\partial\lambda} = \sum_{n\in\mathbf{I}_\text{DC}\setminus\mathbf{I}_\text{cons}} -\frac{\Delta f\chi}{\ln(2)}\frac{\alpha_{5\text{G}-\text{PS}}g_n}{(\lambda+\mu\alpha_{5\text{G}-\text{PS}}g_n)^2} \tag{33}$$

$$\frac{\partial f_1(\mu,\lambda)}{\partial\mu} = \sum_{n\in\mathbf{I}_\text{DC}\setminus\mathbf{I}_\text{cons}} -\frac{\Delta f\chi}{\ln(2)}\frac{(\alpha_{5\text{G}-\text{PS}}g_n)^2}{(\lambda+\mu\alpha_{5\text{G}-\text{PS}}g_n)^2} \tag{34}$$

$$\frac{\partial f_2(\mu,\lambda)}{\partial\lambda} = \sum_{n\in\mathbf{I}_\text{DC}\setminus\mathbf{I}_\text{cons}} -\frac{\Delta f\chi}{\ln(2)}\frac{1}{(\lambda+\mu\alpha_{5\text{G}-\text{PS}}g_n)^2} \tag{35}$$

$$\frac{\partial f_2(\mu,\lambda)}{\partial\mu} = \sum_{n\in\mathbf{I}_\text{DC}\setminus\mathbf{I}_\text{cons}} -\frac{\Delta f\chi}{\ln(2)}\frac{\alpha_{5\text{G}-\text{PS}}g_n}{(\lambda+\mu\alpha_{5\text{G}-\text{PS}}g_n)^2} = \frac{\partial f_1(\mu,\lambda)}{\partial\lambda}. \tag{36}$$

The k-th iterative improvement of λ and μ can be described as

$$\begin{bmatrix}\lambda_{k+1}\\ \mu_{k+1}\end{bmatrix} = \begin{bmatrix}\lambda_k\\ \mu_k\end{bmatrix} - \epsilon\begin{bmatrix}\Delta\lambda_k\\ \Delta\mu_k\end{bmatrix}, \tag{37}$$

where

$$\begin{bmatrix}\Delta\lambda_k\\ \Delta\mu_k\end{bmatrix} = \begin{bmatrix}\frac{\partial f_1(\mu,\lambda)}{\partial\lambda} & \frac{\partial f_1(\mu,\lambda)}{\partial\mu}\\ \frac{\partial f_1(\mu,\lambda)}{\partial\mu} & \frac{\partial f_2(\mu,\lambda)}{\partial\mu}\end{bmatrix}\Bigg|^{-1}_{\mu_k,\lambda_k}\begin{bmatrix}f_1(\mu_k,\lambda_k)\\ f_2(\mu_k,\lambda_k)\end{bmatrix}, \tag{38}$$

and $\epsilon \in \langle 0;1\rangle$ is the update scaling factor. While Newton method guarantees fast convergence, it is important to guarantee that multipliers μ and λ lie within their feasible region, i.e., $\lambda \geq 0$ and $\mu \geq 0$. It is done by the adjustment of ϵ parameter, so that

$$\epsilon_\mu = \begin{cases}\dfrac{\mu_k}{\Delta\mu_k} & \text{for } \Delta\mu_k > 0\\ 1 & \text{for } \Delta\mu_k \leq 0,\end{cases} \tag{39}$$

$$\epsilon_\lambda = \begin{cases}\dfrac{\lambda_k}{\Delta\lambda_k} & \text{for } \Delta\lambda_k > 0\\ 1 & \text{for } \Delta\lambda_k \leq 0,\end{cases} \tag{40}$$

and

$$\epsilon = 0.98\min\left\{1,\epsilon_\mu,\epsilon_\lambda\right\}, \tag{41}$$

where value 0.98 has been chosen to guarantee strict feasibility of the solution. The set of the constrained subcarriers $\mathbf{I}_\text{cons}$ is updated in each iteration. Empirically, λ and μ obtained in the previous iteration can be used in the next one providing fast Newton method convergence.

Thus, the block diagram of our algorithm solving the optimization problem is shown in Fig. 4. First, two simplest cases of μ or λ being equal to zero are solved. If these do not succeed, the Newton method is used to solve the optimization problem for both μ and λ higher than 0. For each case, in the first iteration, the power allocated to each subcarrier is not constrained ($\forall_{n\in\mathbf{I}_\text{DC}}\mu_n = 0$). For the n-th subcarrier having the minimum, negative power out of all subcarriers its power has to be set 0 in the next iteration. It will cause an increase of the interference power and increase of the 5G-system transmit power. Therefore, active state of μ and λ is not changed.

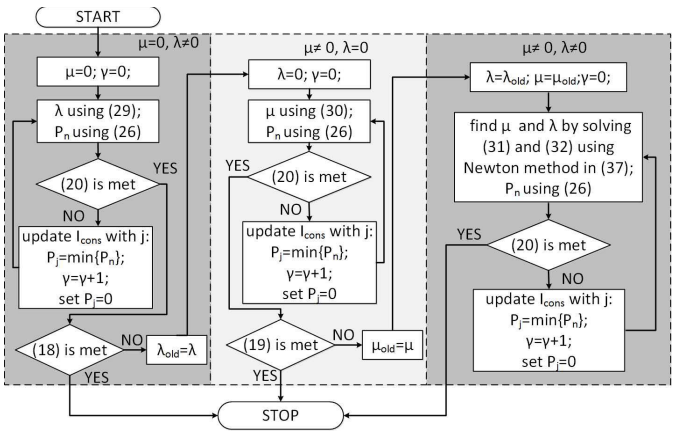

Fig. 4. Block scheme for the solution of optimization problem.

V. Case Study: System Coexistence

The potential of the NC-MC transmission in comparison to the MC transmission with the contiguous subcarriers allocation can be estimated by means of throughput evaluation keeping in mind the constraints on the allowable level of interference induced to PS. The optimization problem and solution presented in Sec. IV is used for 5G system using: a. OFDM, b. NC-OFDM, c. NC-OFDM spectrally shaped at TX using Hanning windowing, and d. NC-FBMC using PHYDYAS filter. For further analysis, we have selected arbitrarily two test scenarios: first, when an operator wants to introduce the NC-MC 5G system in the available frequency bands while maintaining 2G system transmission (GSM) that needs to be protected, and second, when the protected system is the 3G system, UMTS. In each test-case we have made two types of analysis - *a. measurement-based*, where we prove that the proposed interference model used in theoretical analysis is valid, and that NC-MC scheme facilitates coexistence of 5G and PS, and *b. simulation based*, where we calculate the maximum throughput achievable with a given MC scheme using optimization method proposed in Sec. IV-A.

A. System Setup

The PS is assumed to be either GSM or UMTS carrier at frequency 940 MHz or 2130 MHz, respectively. The 5G system is centered at 938.5 MHz or 2128.5 MHz in the presence of these earlier-generation systems, and can utilize the maximum of 600 subcarriers separated by $\Delta f = 15$ kHz, i.e., the maximal occupied bandwidth is 9 MHz. The IFFT size in all considered OFDM-based systems is $N = 1024$. In FBMC, K-times oversampling is assumed. The cyclic prefix in OFDM/NC-OFDM/windowed NC-OFDM system consists of $N_{\mathrm{CP}} = N/16$ samples. The Hanning window extends the NC-OFDM symbol by $N_{\mathrm{w}} = N/16$ samples. The PHYDYAS filter overlapping factor is $K = 4$. Maximal transmit power of the 5G system is 100 mW and the noise figure at 5G UE equals 12 dB. If not stated differently, the transmit power of PS BS is 33 dBm, and the required SIR is 9 dB as defined in [25]. The antenna gains are 15 dBi and 0 dBi for BS and UE, respectively [25]. The pathloss is calculated according to the Log-distance path loss model [26] with pathloss exponent equal to 3. While the frequency response (both at TX and RX) of the NC-MC schemes has been derived in Sec. III, the RX filter characteristic of the GSM receiver has been taken from the ACS characteristic provided in [25], the PSD of GSM transmission has been assumed to be equal to SEM defined in [27], i.e., the worst case scenario has been considered. In case of UMTS, standards [28] and [29] have been used to obtain ACLR and ACS values.

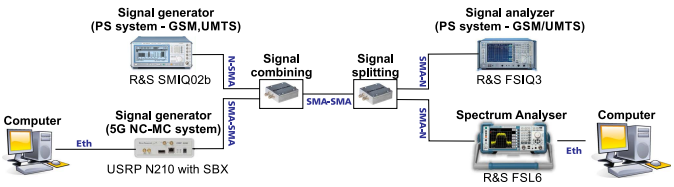

Fig. 5. Measurement setup

B. Protection of GSM Link

Below, we evaluate coexistence of two systems - the 5G NC-MC/OFDM system and GSM (see Fig. 5) by analyzing the power spectral density and observing the mutual interference. The 5G NC-MC signal has been generated using the GNU-Radio software and transmitted using the USRP N210 board equipped with SBX board. The generated 5G NC-MC signal occupies subcarriers $\mathbf{I}_{\mathrm{DC}} = \{-300, \ldots, -1\} \cup \{1, \ldots, 66\} \cup \{134, \ldots, 300\}$ (note the notch of 67 subcarriers corresponding to 1 MHz) with equally distributed power. The standard OFDM uses $\mathbf{I}_{\mathrm{DC}} = \{-300, \ldots, -1\} \cup \{1, \ldots, 300\}$ with equally distributed power.

Moreover, the GSM signal has been generated using the Rohde&Schwarz FSIQ03 Vector Signal Generator. The transmit power has been set to -10 dBm (due to the hardware protection limits), and GMSK modulation with Gaussian filter of $BT = 0.3$ has been used (as defined for GSM). Such two signals (i.e., NC-MC/OFDM and GSM) have been combined in the MiniCircuits ZN2PD2-63-S+ 350-6000 MHz combiner. In order to eliminate the influence of wireless propagation and analyze the interference phenomena between the systems, we have connected the combiner with the 3 dB splitter of the same vendor. Then, the combined signal has been analyzed by the Rohde&Schwarz Spectrum Analyzed FSL6 connected via Ethernet with the PC computer, where the received data have been post-processed. In parallel, the other part of split signal has been received by the Rohde&Schwarz SMIQ02b Signal Analyzer, where analogous GSM reception parameters have been set, and the input filter of 1 MHz bandwidth has been manually selected.

Let us observe the signals PSDs, SEMs and the interference power observed at each subcarrier at the 5G UE receiver as presented in Fig. 6. The noise PSD observed at the spectrum analyzer (SA), is depicted with dashed line. The real (measured) GSM signal (PSD: gray line with stars) generates various interference powers at each subcarrier of MC receiver: higher for OFDM-based RX (grey line with triangles) and lower for FBMC-based RX (grey line with squares).

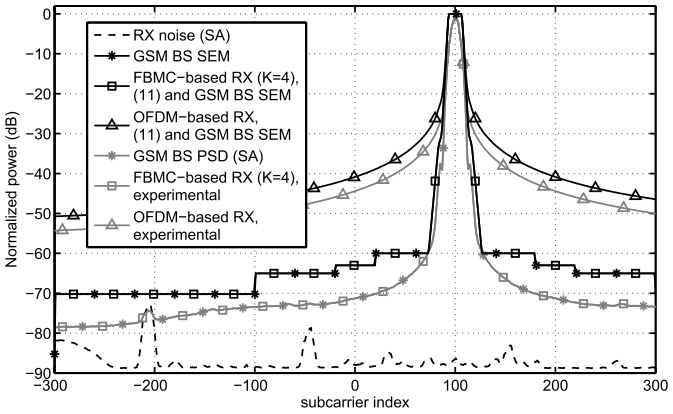

Fig. 6. PSD and SEM of GSM BS signal and interference power caused by these signals at MC RX.

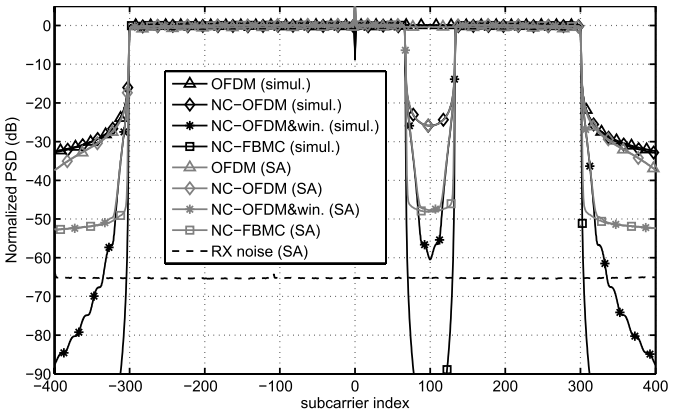

Fig. 7. Power Spectral Density of the 5G signal for PS being GSM.

These interference powers have been obtained running the OFDM/FBMC receiver in post-processing. The *worst case* interference power can be estimated based on GSM BS SEM (black line with stars). This interference power (per subcarrier) is obtained using formula (11) for (NC-)OFDM receiver (black line with stars) and (NC-)FBMC receiver (black line with squares). It is visible that the proposed analytical formula for received interference power, i.e., (11), is coherent with the measurements results. Estimated interference power is typically a few decibels higher than the measured value as a result of *worst case* GSM PSD.

In Fig. 7, we can observe the PSD of the 5G NC-MC and OFDM signals, which are the results of simulations (simul.) and the SA-based reception. Focusing on the frequency gap one can assess the average power of interference induced by the 5G MC transmitter to the GSM band. One can notice that in both cases (of simulations and measurements) the NC-FBMC signal outperforms the traditional NC-OFDM solutions in terms of the power of induced interference. However, application of simple signal processing (Hanning windowing) can significantly improve its performance. Interestingly, for NC-FBMC, the practically achievable OOBE power level is much higher, e.g., about -48 dB, that in the case of PSD generated using simulations, e.g., about -110 dB. It is caused by imperfection of a practical TX and RX realizations, e.g., nonlinearity of an RF front-end causing intermodulation effects [9].

Let us verify if the coexisting 5G NC-MC signal leads to any performance degradation in the legacy GSM system receiver. The error-vector magnitude (EVM) is the justified metric for such performance evaluation. We have set the transmit power in such a way that the total observed power by the PS UE has been -19.2 dBm for the GSM signal, and -29 dBm for 5G signal. First, we have measured the observed EVM at the GSM receiver if there has been no interfering 5G signal, and we have achieved the value of $EVM = 0.85\%$ RMS, what is equivalent to approximately 41 dB of SNR. If we generate the traditional (i.e., contiguous) OFDM signal, which overlaps the GSM signal at PS UE receiver, the observed EVM increases to 12% (SNR $\approx$ 18.3 dB). However, when we have applied the 5G NC-MC signal with 1 MHz gap for GSM protection, the following values of EVM have been achieved: for NC-OFDM case - 1.17% (SNR$\approx$ $38.6dB$), while for NC-OFDM with windowing as well as for NC-FBMC - 0.9% (SNR $\approx$ $40.9dB$). These results show that the NC-MC schemes decrease both interference power in-band of PS (shown in Fig. 7) and effective interference at the PS receiver (the EVM values).

C. Protection of UMTS Users

In our second experiment, we use the same system setup as illustrated in Fig. 5 and most parameters as used in the previous section, but we have adjusted the PS transmit signal parameters to meet the requirements of UMTS standard for downlink transmission. In particular, assuming the root-raised cosine filter of roll-off factor 0.22, we have applied the QPSK data modulation for pseudo-randomly generated data. The center frequency of the 5 MHz signal has been set to 2130 MHz, whereas the central frequency of the NC-MC signal has been set to 2128.5 MHz. The generated 5G NC-MC signal occupies subcarriers of indices in $\mathbf{I}_{\mathrm{DC}} = \{-300, \ldots, -67\} \cup \{267, \ldots, 300\}$ (note a notch of 5 MHz), with equally distributed power. The standard OFDM uses $\mathbf{I}_{\mathrm{DC}} = \{-300, \ldots, -1\} \cup \{1, \ldots, 300\}$ with equally distributed power.

Analogously to the previous case, where the GSM signal has been protected, we demonstrate in Fig. 8 the ACLR (being more strict than SEM) and PSD of the UMTS signal, denoted by black and gray solid lines with stars, respectively. The *worst case* interference power received on a given 5G NC-MC system subcarrier is denoted by black line with rectangles and triangles for (NC-)FBMC and (NC-)OFDM, respectively. It has been obtained using ACLR limits defined for UMTS BS and (11). The experimental UMTS BS signal has been post-processed using (NC-)OFDM and (NC-)FBMC receivers to obtain interference powers observed at each subcarrier (gray lines with triangles and squares for OFDM and FBMC, respectively). Similarly as in Fig. 6, the analytical interference model using ACLR defined for UMTS BS and (11) constitutes an upper-bound of

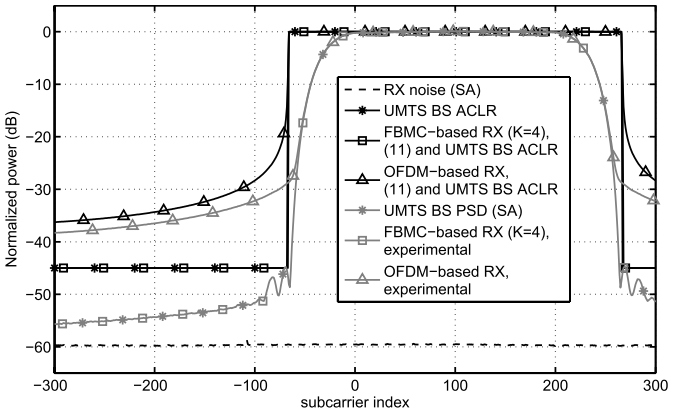

Fig. 8. PSD and SEM of UMTS BS signal and interference power caused by these signals at MC RX.

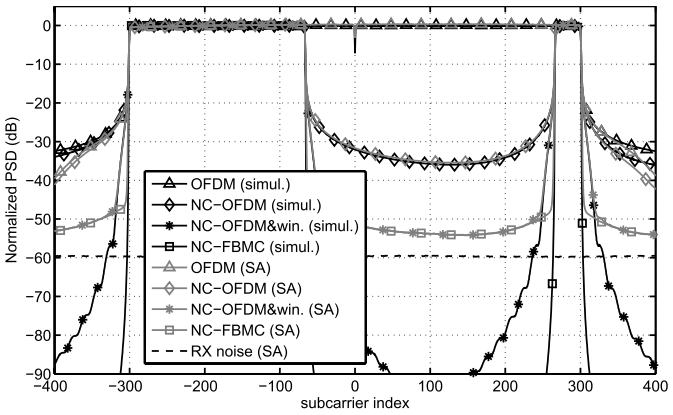

Fig. 9. Power Spectral Density of the 5G signal for PS being UMTS.

interference observed during a real transmission. In Fig. 9, the PSDs for various 5G NC-MC and OFDM signals are shown. It is visible that the lowest OOBE-power level is achieved in case of computer simulations by the NC-FBMC signal, i.e., software-generated NC-FBMC. Although, at the SA, the PSD obtained by means of NC-OFDM windowing has similar results, the other schemes (NC-OFDM and OFDM), introduce much stronger interference to the PS band.

Because it has not been possible to measure the characteristic of the built-in filters of the UMTS test receiver, again, we have measured the EVM of the received signal by PS UE to assess its reception quality in the presence of coexisting 5G NC-MC or OFDM signals. The received power has been equal to -31 dBm for the UMTS signal, and -42 dBm for the 5G NC-MC/OFDM signal. First, as the reference, the EVM of the UMTS signal with no interference has been measured resulting in 1.45% RMS that corresponds to SNR of 36.8 dB. Then, when the traditional (with contiguous subcarriers) OFDM signal has been transmitted, the observed EVM has been equal to 22% RMS (SNR$\approx$13 dB). However, when the non-contiguous scheme has been applied, there have not been any problems with signal synchronization observed, and the values of EVM have been as follows: 1.6% RMS (SNR$\approx$35.9 dB) for NC-OFDM, and 1.48% RMS (SNR$\approx$36.6 dB) for both NC-OFDM with windowing and NC-FBMC. The achieved results have proved the correctness of the interference model applied in our paper and usefulness of the NC-MC system for increasing spectrum utilization.

D. Throughput and Outage Evaluation

So far, we have proved that although various 5G MC schemes utilize various pulse shapes (resulting in various inter-system interference coupling), the effective interference both at PS RX and 5G RX can be modeled using the approach proposed in Sec. III. Let us now evaluate the mean rate limits that could be achieved by the mobile 5G-system users applying NC-MC or OFDM schemes in realistic scenario where the influence of transmission channel is considered. In particular, the effects of multipath propagation, Doppler shifts, and control information delay are taken into account. The multipath fading channel is 9-path Extended Vehicular A model [30] generated independently for each of the considered paths. In practice, 5G BS would struggle to maximize throughput while protecting PS (using the algorithm presented in Sec. IV-A) as the Channel State Information (CSI) could be outdated/delayed or limited/quantized. Because of users mobility all channels frequency responses change with the terminals velocities and the Doppler frequencies. While 5G BS gets direct CSI reports from 5G EU, the measurements carried by PS UE are relayed by PS BS. Thus, in our model, 5G BS utilizes CSI of channels c and b (as shown in Fig. 3) delayed by 5 ms. CSIs of channels a and d are assumed to be perfectly known at 5G BS. Observe that this delay has no impact on the mean throughput in the 5G-5G link (in comparison to the full CSI knowledge from all paths at 5G BS), but the resultant power allocation can violate the PS SIR limit. On the other hand, limited CSI means that 5G BS knows only the pathloss components, i.e., α_{5G-PS}, α_{5G-5G}, α_{PS-PS}, α_{PS-5G}, not the channel frequency response. This is a more delay-tolerant approach that needs much less control information to be collected by 5G BS. Hereafter we use the following notation: phrase *perfect* represents the case with ideal TX and RX filters, e.g., no OOBE, *limited* refers to the limited CSI, whereas *delayed* stands for a case where 5 ms delay is considered in reporting CSI by PS.

The parameters presented in Sec. V-A have been used as an input for the optimization problem defined in Sec. IV. The considered distances between PS BS and PS UE, PS BS and 5G UE, 5G BS and 5G UE are equal to 2 km, 2 km, 100 m, respectively. The mean throughputs (over 10^4 channel realizations) of the 5G NC-MC and OFDM links in the presence of GSM being PS are presented in Fig. 10. It is visible that PHYDYAS filters with $K = 4$ are selective enough, both at the transmitter and at the receiver to obtain nearly maximal throughput (i.e., the curve representing throughput for the 5G system using *perfect* TX/RX filter overlaps the curve for FBMC case). However, decreased overlapping factor, i.e., $K = 2$, causes stronger interference to GSM UE, degrading 5G system throughput, especially when GSM UE is close to 5G BS. In the case of NC-OFDM-based 5G system, its BS has to be distanced by at least 78 m from GSM

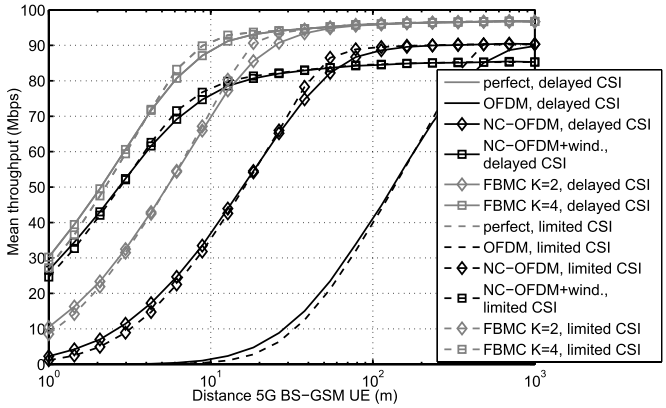

Fig. 10. Throughput obtained with different MC schemes while protecting GSM UE.

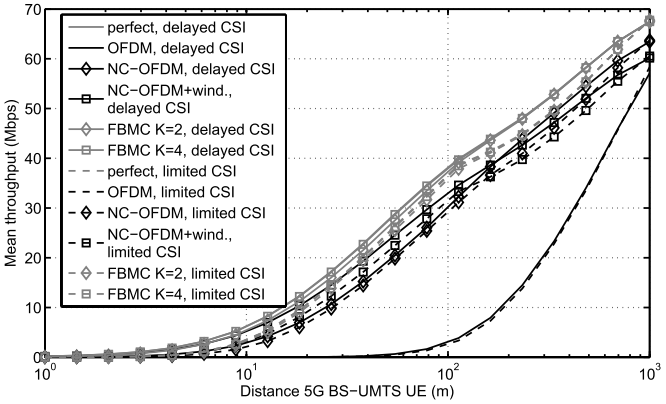

Fig. 11. Throughput obtained with different MC schemes while protecting UMTS UE.

UE to obtain more than 90% of the maximal throughput. However, NC-OFDM can be improved by some additional spectrum shaping, like windowing. In this case, the achievable throughput is significantly increased when the system is limited by interference caused to GSM system (small 5G BS-GSM UE distance). Utilization of standard OFDM requires 5G BS to be distanced by more than 350 m from GSM UE in order to achieve at least 90% of the *perfect*-case throughput. In the case of NC-OFDM/OFDM, the maximal achievable throughput equals $N/(N + N_{\mathrm{CP}}) \approx 0.94$ of the *perfect* case because of the application of CP. Most importantly, the result for FBMC utilizing all subcarriers with the same allocated power would be similar to the ones of OFDM system, i.e., non-contiguity of the MC scheme is a key requirement to improve throughput. Observe that in the considered scenario, both limited and delayed CSI utilization provide similar throughput. In standard, *water-filling* power allocation the *delayed* CSI scheme should utilize the knowledge on frequency-selective fading coefficients, and should be no worse than *limited*-CSI case. Here, the throughput in the *limited*-CSI case exceeding the throughput in the *delayed*-CSI case is possible at the cost of increased interference to PS.

In order to map the achievable throughput to services available to network users, let us consider the VoIP service using Adaptive Multi-Rate (AMR) voice-coder utilizing 12.2 kbps. It can be assumed that 98% of frames has to be delivered to users for sufficient service quality [31]. Thus, the maximal number of users N_{u} that can be served is $N_{\mathrm{u}} = \max_n Pr(R < n12.2kbps) = 10^{-2}$ where R is a random variable of the throughput. The network capacity is not specified by the means of throughput, but by its 2nd percentile. For the distance between PS UE and 5G BS equal to 100 m, assuming *delayed*-CSI case, the maximal number of VoIP calls to be served is 6713, 6711, 6701, 5895, 5717, and 709 for the *perfect* TX/RX filters, FBMC with $K = 4$, FBMC with $K = 2$, NC-OFDM with windowing, NC-OFDM, and OFDM, respectively. All NC-MC schemes outperform standard OFDM significantly.

Similarly, the achievable throughput in the case of UMTS being PS can be calculated. The utilized parameters are the same as defined in Sec. V-A. In Fig. 11, it is visible that UMTS limits the achievable 5G throughput much more than GSM system. Is is mostly caused by small bandwidth of 5G-available spectrum, not utilized by PS. Interestingly, all considered NC-MC systems achieve at least about 75% of the maximal possible throughput (the case of *perfect* filters). The standard OFDM obtains much smaller throughput that again confirms the potential of NC-MC schemes. Let us now concisely exemplify, how the achieved throughput can be translated into the delivery of a given service to end-user. We use this as another measure characterizing the proposed solutions. Similarly as for GSM, VoIP service can be considered in 5G system. Using the same assumptions as previously, the maximal number of VoIP calls served is 2145, 2131, 2064, 1830, 1540, and 35 for *perfect* TX/RX filters, FBMC with $K = 4$, FBMC with $K = 2$, NC-OFDM with windowing, NC-OFDM, and OFDM, respectively.

In addition to the estimation of 5G link conditions, outage analysis of PS has been carried for the parameters as above and fixed distance between 5G BS and PS UE equal to 100 m. It is reasonable to define outage SIR to be a few dB below the optimization SIR equal here 9 dB and used in constraint (18). Assume that outage occurs when SIR$<$ 3 dB. Fig. 12 shows the outage probabilities for both PSs (GSM and UMTS) and all considered MC schemes while varying the UE velocity (impacting the wireless channel dynamics). It is visible that for slowly moving UEs, the delay in CSI reporting enables the 5G system to protect the PSs transmissions. Unfortunately, for higher UEs speed the *delayed* CSI results in high outage probability. It is a result of 5G BS allocating relatively high power to subcarriers, overlapping spectrum occupied by PS. After 5 ms the channel frequency response changes, resulting in PS SIR exceeding outage threshold. This phenomenon comes into play the more selective filters are used by a given MC scheme, e.g., for *perfect* TX/RX filters case obtains visibly highest outage probability in UMTS. Such frequency-selective filters provoke the MC systems to utilize faded frequencies in-band of PS. The *limited*-CSI scheme is independent from Rayleigh fading dynamics as it does not consider channels frequency response while performing optimization. While this scheme is the worse for small UEs velocities, it seems to be a

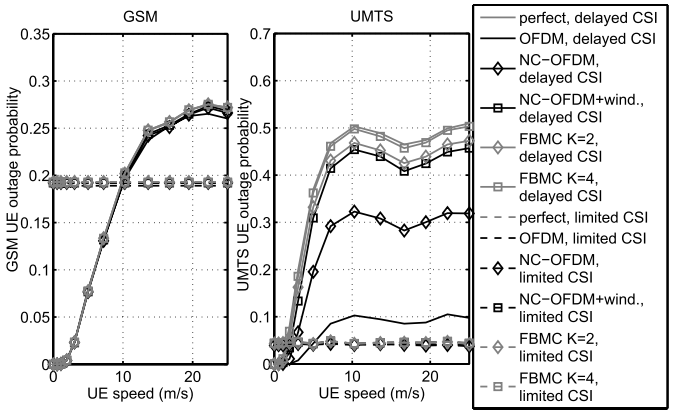

Fig. 12. Probability of PS UE outage (SIR< 3 dB), for various MC schemes. Limited- and delayed-CSI available at 5G BS.

practical solution for power allocation under high users mobility. Additionally, this scheme requires less control information to be collected by the 5G BS.

E. Computational Complexity Analysis

The computational complexity of solving the optimization problem defined in Sec. IV is significantly reduced thanks to the algorithm shown in Fig. 4. Instead of considering $2^{N_\mathrm{d}+2}$ combinations of KKT multipliers being either active or inactive, only the maximum of $3N_\mathrm{d}$ combinations have to be considered. The rationale behind this reduction is shown in Sec. IV-A. Let us assume that P_{In}^{RX} and g_n values are obtained by means of numerical integration using rectangle method with Z subintervals. The algorithm uses the more iterations the more μ_n multipliers have to be activated. In the worst case scenario, all three parts of the algorithm, i.e., for $\mu = 0$ and $\lambda > 0$, for $\mu > 0$ and $\lambda = 0$, and for $\mu > 0$ and $\lambda > 0$, have to be run till γ values of μ_n are activated. For both λ and μ multipliers being positive, Newton method is used to solve equations (31) and (32) using approximately L iterations. Finally, the approximate number of real additions/subtractions is $N_\mathrm{d}(2Z+6L\gamma+6\gamma+6L+13)-3L\gamma^2+4L\gamma-3\gamma^2+\gamma+7L$, the number of multiplications/divisions is $N_\mathrm{d}(6Z+6L\gamma+6\gamma+6L+13)-3\gamma^2-3L\gamma^2+10L\gamma+13L+2$, while the number of comparisons is $3(\gamma+1)\left(N_d-\frac{\gamma}{2}\right)$. Assuming $N = 1024$, $N_\mathrm{d} = 600$ (as in the previous sections), $Z = N$, $\gamma = 13$ (zeroed subcarriers span the bandwidth of a single GSM carrier) and $L = 6$, the maximal number of all operations is 5 648 256. This algorithm can be evaluated using 20 GFLOP signal processor, e.g., C66x from Texas Instruments, with execution time below 1 ms. As such it could be possibly run in real-time in 5G BS.

VI. Discussion and Conclusion

In this position paper, we have examined the feasibility of the small-scale spectrum aggregation and sharing, where - in contrast to the well-known carrier aggregation schemes already applied in 3GPP standards - even very narrow and non-contiguous frequency subbands can be utilized by a single user. Such a non-contiguous nature of the utilized spectrum entails the natural selection of various multicarrier transmission schemes, which are considered as the main candidates for 5G systems. Based on this observation, we have proposed the interference model and identified the rate optimization problem for the 5G NC-MC system link, which has been solved for certain set of constraints. In order to evaluate the correctness of our interference model the experiments with the practical TX and RX hardware have been conducted, where two kinds of systems (narrowband - GSM, and wideband, spread spectrum - UMTS) have been protected. The achieved results justify our interference model. Therefore, it has been applied to calculate the theoretical limits of possible achievable rates in the future 5G NC-MC system. These theoretical results have been confirmed by the computer simulation. Hence, it can be then concluded that the small-scale spectrum aggregation can be considered as a potential solution for future wireless networks.

In our work, we have arbitrarily selected two types of legacy systems: GSM and UMTS. This selection has been made to illustrate the possibility of smooth transition of the frequency assignment from older to newer technologies while keeping the electromagnetic compatibility with the legacy systems. However, the proposed small-scale spectrum aggregation and sharing can also be applied in other, even completely different schemes.

References

[1] Cisco, San Jose, CA, USA. (Feb. 2016). *Cisco Visual Networking Index: Global Mobile Data Traffic Forecast Update, 2015–2020*. [Online]. Available: http://www.cisco.com/c/en/us/solutions/collateral/service-provider/visual-networking-index-vni/mobile-white-paper-c11-520862.pdf

[2] 5G PPP, "What will the 5G-infrastructure-PPP deliver?" 5G PPP, Tech. Rep., accessed on Apr. 4, 2016. [Online]. Available: https://5g-ppp.eu/kpis/

[3] J. G. Andrews *et al.*, "What will 5G be?" *IEEE J. Sel. Areas Commun.*, vol. 32, no. 6, pp. 1065–1082, Jun. 2014.

[4] D. López-Pérez, M. Ding, H. Claussen, and A. H. Jafari, "Towards 1 Gbps/UE in cellular systems: Understanding ultra-dense small cell deployments," *IEEE Commun. Surveys Tut.*, vol. 17, no. 4, pp. 2078–2101, 4th Quart., 2015.

[5] M. Mustonen, M. Matinmikko, M. Palola, S. Yrjýlý, and K. Horneman, "An evolution toward cognitive cellular systems: Licensed shared access for network optimization," *IEEE Commun. Mag.*, vol. 53, no. 5, pp. 68–74, May 2015.

[6] A. Kliks, O. Holland, A. Basaure, and M. Matinmikko, "Spectrum and license flexibility for 5G networks," *IEEE Commun. Mag.*, vol. 53, no. 7, pp. 42–49, Jul. 2015.

[7] I. Sugathapala, I. Kovacevic, B. Lorenzo, S. Glisic, and Y. Fang, "Quantifying benefits in a business portfolio for multi-operator spectrum sharing," *IEEE Trans. Wireless Commun.*, vol. 14, no. 12, pp. 6635–6649, Dec. 2015.

[8] J. Mitola and G. Q. Maguire, Jr., "Cognitive radio: Making software radios more personal," *IEEE Pers. Commun.*, vol. 6, no. 4, pp. 13–18, Apr. 1999.

[9] H. Bogucka, P. Kryszkiewicz, and A. Kliks, "Dynamic spectrum aggregation for future 5G communications," *IEEE Commun. Mag.*, vol. 53, no. 5, pp. 35–43, May 2015.

[10] P. Kryszkiewicz and H. Bogucka, "Out-of-band power reduction in NC-OFDM with optimized cancellation carriers selection," *IEEE Commun. Lett.*, vol. 17, no. 10, pp. 1901–1904, Oct. 2013.

[11] H. Yamaguchi, "Active interference cancellation technique for MB-OFDM cognitive radio," in *Proc. 34th Eur. Microw. Conf.*, vol. 2. Oct. 2004, pp. 1105–1108.

[12] P. Kryszkiewicz, H. Bogucka, and A. M. Wyglinski, "Protection of primary users in dynamically varying radio environment: Practical solutions and challenges," *EURASIP J. Wireless Commun. Netw.*, vol. 2012, no. 1, p. 23, 2012. [Online]. Available: http://jwcn.eurasipjournals.com/content/2012/1/23

[13] T. Weiss, J. Hillenbrand, A. Krohn, and F. K. Jondral, "Mutual interference in OFDM-based spectrum pooling systems," in *Proc. IEEE 59th Veh. Technol. Conf. (VTC-Spring)*, vol. 4. May 2004, pp. 1873–1877.
[14] B. Farhang-Boroujeny, "OFDM versus filter bank multicarrier," *IEEE Signal Process. Mag.*, vol. 28, no. 3, pp. 92–112, May 2011.
[15] J. Yli-Kaakinen and M. Renfors, "Fast-convolution filter bank approach for non-contiguous spectrum use," in *Proc. Future Netw. Mobile Summit (FutureNetworkSummit)*, Jul. 2013, pp. 1–10.
[16] M. Bellanger, *et al.*, "FBMC physical layer: A primer," PHYDYAS, Tech. Rep., Jun. 2010, pp. 1–31.
[17] G. Fettweis, M. Krondorf, and S. Bittner, "GFDM—Generalized frequency division multiplexing," in *Proc. IEEE 69th Veh. Technol. Conf. (VTC Spring)*, Apr. 2009, pp. 1–4.
[18] V. Vakilian, T. Wild, F. Schaich, S. ten Brink, and J. F. Frigon, "Universal-filtered multi-carrier technique for wireless systems beyond LTE," in *Proc. IEEE Globecom Workshops (GC Wkshps)*, Dec. 2013, pp. 223–228.
[19] X. Zhang, M. Jia, L. Chen, J. Ma, and J. Qiu, "Filtered-OFDM—Enabler for flexible waveform in the 5th generation cellular networks," in *Proc. IEEE Global Commun. Conf. (GLOBECOM)*, Dec. 2015, pp. 1–6.
[20] D. Schafhuber, G. Matz, and F. Hlawatsch, "Pulse-shaping OFDM/BFDM systems for time-varying channels: ISI/ICI analysis, optimal pulse design, and efficient implementation," in *Proc. 13th IEEE Int. Symp. Pers., Indoor Mobile Radio Commun.*, vol. 3. Sep. 2002, pp. 1012–1016.
[21] W. Kozek and A. F. Molisch, "Nonorthogonal pulseshapes for multicarrier communications in doubly dispersive channels," *IEEE J. Sel. Areas Commun.*, vol. 16, no. 8, pp. 1579–1589, Oct. 1998.
[22] A. Kliks, I. Stupia, V. Lottici, F. Giannetti, and F. Bader, "Generalized multi-carrier: An efficient platform for cognitive wireless applications," in *Proc. 8th Int. Workshop Multi-Carrier Syst. Solutions (MC-SS)*, May 2011, pp. 1–5.
[23] T. A. Weiss and F. K. Jondral, "Spectrum pooling: An innovative strategy for the enhancement of spectrum efficiency," *IEEE Commun. Mag.*, vol. 42, no. 3, pp. S8–S14, Mar. 2004.
[24] D. P. Bertsekas, *Nonlinear Programming*. Belmont, MA, USA: Athena Scientific, 1999.
[25] CEPT, "Compatibility study for LTE and WiMAX operating within the bands 880–915 MHz/925–960 MHz and 1710–1785 MHz/1805–1880 MHz (900/1800 MHz bands)," CEPT, CEPT Rep., Nov. 2010, pp. 1–81.
[26] T. S. Rappaport, *Wireless Communications: Principles and Practice*, 2nd ed. Upper Saddle River, NJ, USA: Prentice-Hall, 2001.
[27] *Digital Cellular Telecommunications System (Phase 2+); Radio Transmission and Reception*, document ETSI TS 5.05, Mar. 1996.
[28] *User Equipment (UE) Radio Transmission and Reception (FDD)*, document TS 25.101, 3rd Generation Partnership Project, Sep. 2008. [Online]. Available: http://www.3gpp.org/ftp/Specs/html-info/25101.htm
[29] *Base Station (BS) Radio Transmission and Reception (FDD)*, document TS 25.104, 3rd Generation Partnership Project, Sep. 2008. [Online]. Available: http://www.3gpp.org/ftp/Specs/html-info/25104.htm
[30] *Evolved Universal Terrestrial Radio Access (E-UTRA); Base Station (BS) Radio Transmission and Reception*, document TS 36.104, 3rd Generation Partnership Project, May 2008. [Online]. Available: http://www.3gpp.org/ftp/Specs/html-info/36104.htm
[31] *Physical Layer Aspects for Evolved Universal Terrestrial Radio Access (UTRA)*, document TS 25.814, 3rd Generation Partnership Project, Sep. 2006. [Online]. Available: http://www.3gpp.org/ftp/Specs/html-info/25814.htm

Paweł Kryszkiewicz received the M.Sc. and Ph.D. degrees (Hons.) in telecommunications from the Poznan University of Technology (PUT), Poland, in 2010 and 2015, respectively. He is currently an Assistant Professor with the Chair of Wireless Communications, PUT. He was involved in a number of national and international projects, such as FP7 cognitive radio systems for efficient sharing of TV white spaces in European context, Network of Excellence in Wireless Communications from 2012 to 2015, and advanced coexistence technologies for radio optimisation and unlicensed spectrum. Since 2015, he has been involved in H2020 Project COHERENT. His main field of interest are problems concerning the physical layer of the cognitive radio system, multicarrier signal design for green communications, and interference limitation in 5G systems.

Adrian Kliks received the M.Sc. and Ph.D. degrees (Hons.) in telecommunications from the Poznan University of Technology (PUT), Poland, in 2005 and 2011, respectively. He is currently an Assistant Professor with the Chair of Wireless Communications, PUT. He was involved in various industrial and international research projects. His scientific interests include i.a. advanced multicarrier communications, waveform design, small-cells in heterogeneous networks, WiFi offloading, and cognitive radio.

Hanna Bogucka received the Ph.D. and Doctor Habilitus degrees in telecommunications from the Poznan University of Technology (PUT), Poznan, Poland, in 1995 and 2006, respectively. She is currently a Full Professor and the Deputy-Dean for Research with the Faculty of Electronics and Telecommunications, PUT. She is involved in research in wireless communications, cognitive radio and energy-efficient wireless systems and networks. She has been involved in the projects funded by the Polish National Science Centre, Ministry of Science and Higher Education, and has been a Consultant with the Polish Telecomunication Operator. She has been involved in multiple European 5th 7th Framework Programme and Horizon 2020 projects dealing with novel flexible and cognitive radio technologies. She has authored over 150 papers, and published in major IEEE journals and magazines, European journals, and the proceedings of international conferences. She is also the author of one book and a number of book chapters focusing on green communications and cognitive radio. She was the IEEE Communications Society Director of the EAME Region (Europe, Africa, and Middle East) from 2014 to 2015 and the IEEE Radio Communication Committee Chair from 2015 to 2016.